UCRL-JC-122507
PREPRINT

# Spray Cooling Heat-Transfer with Subcooled Trichlorotrifluoroethane (Freon-113) for Vertical Constant Heat Flux Surfaces

C. Matthew Kendall, Lawrence Livermore National Laboratory
and Jack P. Holman, Sothern Methodist University

This paper was prepared for submittal to the
1996 International Mechanical Engineering Congress and Exposition
Atlanta, Georgia
November 18-20, 1996

June 6, 1996

Lawrence Livermore National Laboratory

DISCLAIMER

DISCLAIMER

**Portions of this document may be illegible in electronic image products. Images are produced from the best available original document.**

# SPRAY COOLING HEAT-TRANSFER WITH SUBCOOLED TRICHLOROTRIFLUOROETHANE (FREON-113) FOR VERTICAL CONSTANT HEAT FLUX SURFACES


**C. Matthew Kendall**
Lawrence Livermore National Laboratory
Livermore, California 94550, U.S.A.

**Jack P. Holman**
Southern Methodist University, Mechanical Engineering Department,
Dallas, Texas 75275-0335, U.S.A.



## ABSTRACT

Experiments were conducted using subcooled trichlorotrifluoroethane (Freon-113) sprayed vertically downward through vertical constant heat flux surfaces. Both local and average heat-transfer behaviors were investigated for Freon-113 sprays with 40°C of subcooling, droplet sizes ranging from 200 μm to 1250 μm, and droplet breakup velocities ranging from 5 m/s to 29 m/s. Full-cone type nozzles were used to generate the spray. Test assemblies consisted of one to six 7.62 cm by 7.62 cm vertical constant heat flux surfaces which were parallel with respect to each other and aligned horizontally. The distance between the heated surfaces was varied from 6.35 mm to 76.2 mm. Steady state heat fluxes as high as 13 W/cm$^2$ were achieved. A dependence on the surface distance from the axial centerline of the spray was found. For surfaces sufficiently removed from the centerline, the local and average heat-transfer behaviors were identical and correlated by a power relation of the form seen for normal-impact sprays which involves the Weber number, a nondimensionalized temperature difference, and a mass flux parameter. For surfaces closer to the centerline, the local heat-transfer was dependent on the vertical location on the surface while the average heat-transfer was described by a semi-log correlation involving the same parameters. The heat-transfer behavior was independent of the distance (gap) between the heated surfaces for the gaps investigated.


## NOMENCLATURE

| | |
|---|---|
| A | heat-transfer area, m$^2$ |
| B | constant of equation (9) |
| c | specific heat per unit mass, J kg$^{-1}$ °C$^{-1}$ |
| d | nozzle orifice diameter, m |
| $d_p$ | droplet diameter, m |
| E | voltage drop across precision resistor, V |
| e | voltage drop across individual test surface, V |
| gap | distance between parallel vertical constant heat flux surfaces |

| | |
|---|---|
| $h_{fg}$ | enthalpy of vaporization, J kg$^{-1}$ |
| M | molecular weight, g mol$^{-1}$ |
| P | parachor, cm$^3$ g$^{0.25}$ s$^{-0.5}$ mol$^{-1}$ |
| q" | heat flux, W m$^{-2}$ |
| $R_p$ | resistance of precision resistor, Ohm |
| T | temperature, °C |
| v | droplet breakup velocity, m s$^{-1}$ |
| $v_l$ | liquid velocity prior to the nozzle, m s$^{-1}$ |
| We | Weber number, $\rho_l v^2 d_p \sigma^{-1}$ |
| x | distance from nozzle to heat surface, m |
| Y | distance from the axial centerline of the spray, m |

## Greek

| | |
|---|---|
| $\beta$ | nozzle spray angle, radians |
| $\Delta p$ | pressure difference across nozzle, Pa |
| $\Delta T$ | temperature difference, $T_w$-$T_l$, °C |
| $\gamma$ | exponent of equation (9) |
| $\mu$ | viscosity, kg m$^{-1}$ s$^{-1}$ |
| $\rho$ | density, kg m$^{-3}$ |
| $\sigma$ | surface tension, N m$^{-1}$ |

## Subscripts

| | |
|---|---|
| avg | average of all test surfaces |
| conduction | conduction losses |
| f | film |
| l | liquid |
| power | electric heat input |
| radiation | radiation losses |
| v | vapor |
| x | local surface value |
| w | test surface |

## INTRODUCTION

One of the limiting design elements of electronic systems is the ability to effectively remove heat and maintain low operating temperatures (less than 85 °C). These systems, with high power chips packed close together, present a significant thermal challenge to the design engineer. In many situations, conventional convective cooling can not provide high heat fluxes and low uniform surface temperatures. Spray cooling with dielectric fluids may be a suitable cooling design choice because of the high heat fluxes obtainable while maintaining relatively low uniform surface temperatures, and the ability to effectively cool localized areas. Extensive spray cooling heat-transfer research has been performed using normally impacting sprays. This research has been extended to practical applications by investigators such as Tilton et al. (1992) and Chang et al. (1993), who successfully demonstrated the suitability of spray cooling for simulated electronic multi-chip modules.

Many electronic systems, however, incorporate stacked multi-chip array substrates which eliminate normally impacting sprays as a cooling alternative because of their geometry. Spray cooling may still be a viable thermal management design alternative for these geometries, but a better understanding of the heat-transfer behavior for low impact angle sprays (less than 10 degrees measured from the surface) is needed. A few authors such as Ghodbane (1988) and Sehmbey et al. (1992) have investigated the heat-transfer effect of varying the impact angle of a spray. Although their results provide insight, they do not quantify the heat transfer behavior. The purpose of this investigation was to gain an understanding in the heat-transfer mechanisms sprays in vertical constant heat flux (VCHF) surfaces using subcooled Freon-113 and obtain a nondimensional correlation of heat flux using the surface and spray parameters.

## EXPERIMENTAL METHOD

The experimental apparatus, shown schematically in Figure 1, was designed to provide a steady, constant temperature flow of subcooled Freon-113 to the test chamber. Figure 2 provides more detail of the Freon-113 closed loop. The test chamber in Figures 1 and 2 is 40.64 cm wide, 40.64 cm tall, and 96.52 cm long with Plexiglas access windows for experimental observations and flow visualization. A single commercially available, pressure atomizing, full-cone type nozzles was used to spray vertically downward through heated test surfaces. Four different nozzles were used in the experiments. A multiple degree-of-freedom alignment frame was used to position the test assembly in the chamber.

Figure 3 illustrates a typical assembly, which consisted of one to six equally spaced parallel test surfaces separated by alternating copper and Teflon spacing bars which formed a serpentine pattern, connecting the test surfaces electrically in series. Four surface spacing distances were employed in the investigation ranging from 6.35 mm to 25.4 mm. Four 6.35 mm steel all-thread bars in Teflon sleeves held the test surfaces and spaces bars together, as well as secured the assembly to the alignment frame. Test surfaces were constructed of 0.127 mm thick 316 stainless steel shim stock and had two 7.62 cm by 7.62 cm (58.1 $cm^2$) exposed surfaces for heat-transfer. Three 0.127 mm type E, chromel-constantan wire thermocouples were attached to each test surface using a high thermal conductivity epoxy at the locations indicated in Fig. 4. Another assembly with a single heated surface was also tested in the experiments. The purpose of the single surface assembly was to remove possible multiple surface interaction effects while evaluating the heat-transfer behavior. To maintain the effect of the space bars seen in the multiple surface assemblies, 38.1 mm of space bars were extended on both sides of the single surface. Eight 0.127 mm type E, chromel-constantan wire thermocouples were attached to the single test surface at the locations indicated in Fig. 5. In all cases, the thermocouples were located on the side of the test surface facing away from the axial centerline of the spray (i.e. the thermocouples were not the direct droplet path). Thermocouple wires were placed in a tension clamp below the test assembly to minimize their effect on the droplet flow. The measured variation of the thermocouple readings at room temperature and in the ice bath was $\pm$ 0.1°C.

### Testing Procedure

The test surfaces were thoroughly cleaned and installed, and then the test chamber was sealed. The three cooling loops were activated and the Freon-113 temperature was allowed to cool down to the subcooled testing temperature, which ranged from 0 °C to 10 °C. When steady flow conditions were achieved, the electrical heating system was activated and initial zero-power temperature and voltage readings were taken. Test surface wall temperatures were varied by progressively increasing the voltage drop across each surface. Thermocouple readings, pressure readings, and voltage readings were recorded on a data logger for each incremental power setting. During testing, the measured chamber pressure was 14.7 $\pm$ 1.0 psia corresponding to a saturation temperature of 48°C $\pm$ 2°C. Experiments were terminated when a data-logging system detected the initiation of a local burnout (rapid rise in the local wall temperature). Test surfaces were visually inspected after each experiment was terminated and replaced if necessary. This sequence was repeated until the entire flow range of each nozzle was tested.

## DATA ANALYSIS

The physical quantities and parameters which influence heat-transfer in normally impacting sprays were anticipated to play a similar role in VCHF surface spray cooling. In addition, the separation distance between the heated surfaces was also expected to influence the heat-transfer. Therefore, the heat-transfer behavior was expected to be influenced by the liquid and surface temperatures, Freon-113 properties, droplet diameter, droplet breakup velocity, distances from the nozzle exit to the heated surface, and separation distance between the heated surfaces. A summary of the experimental range of the test parameters is presented

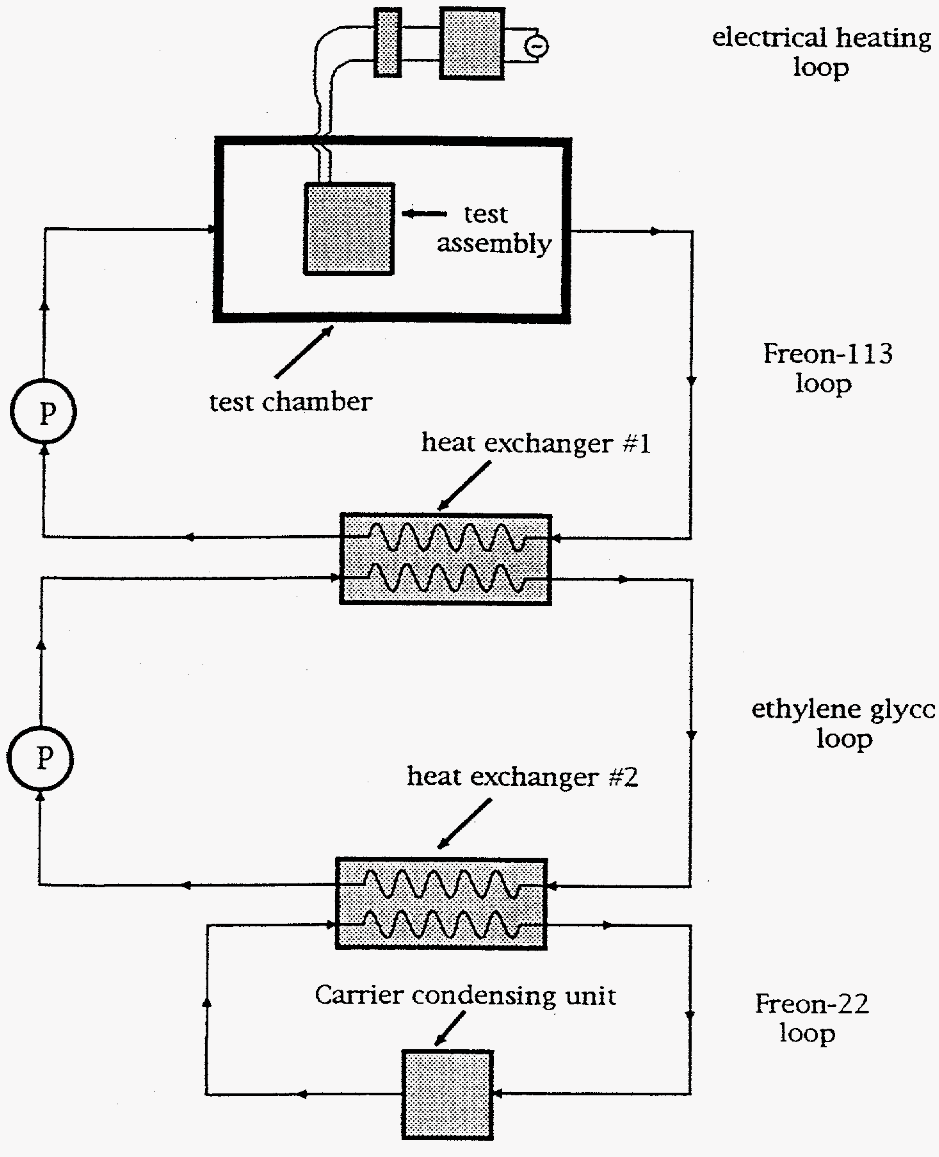


**Figure 1 Schematic Diagram of the Experimental Apparatus**

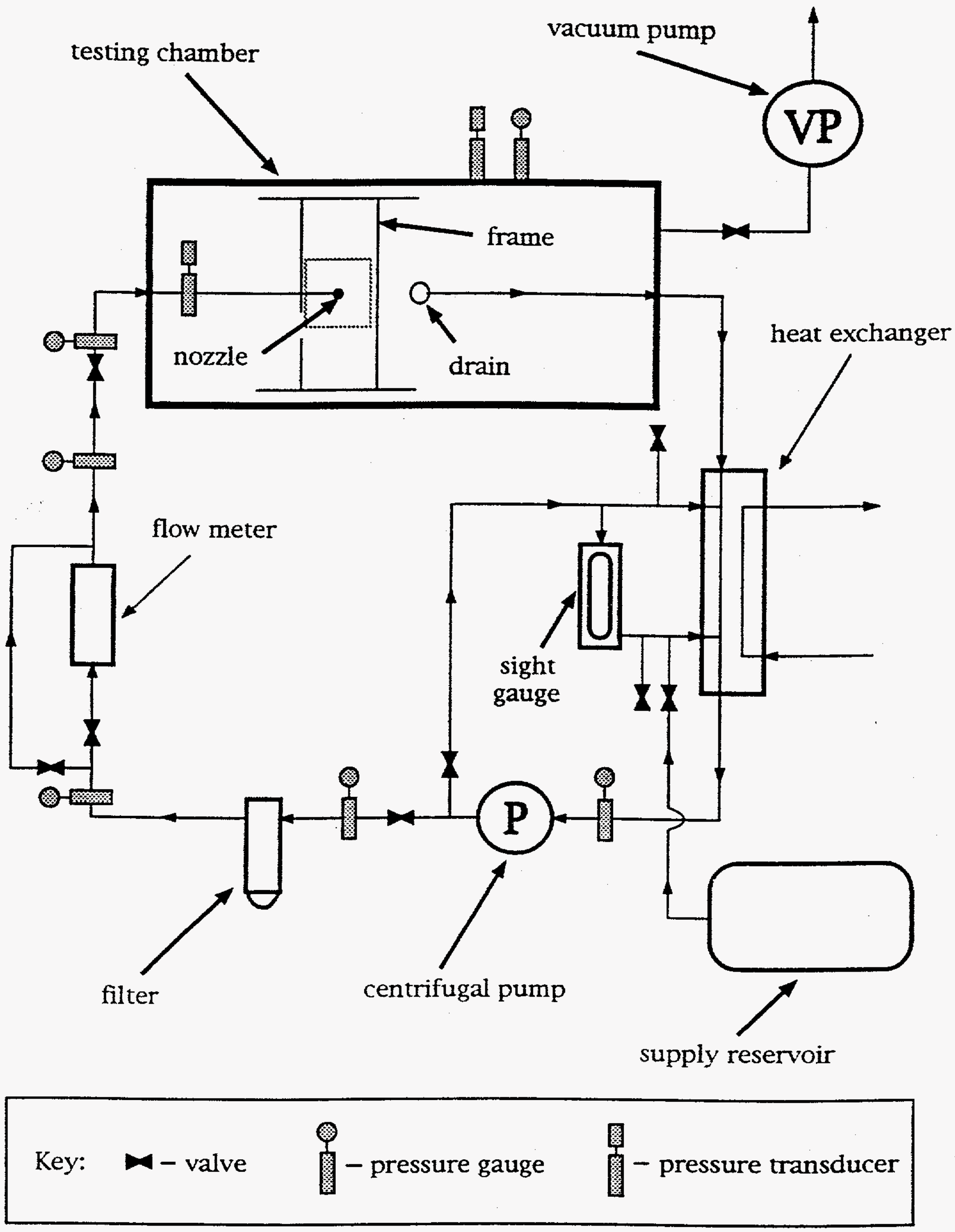


**Figure 2 Freon-113 Closed Loop**

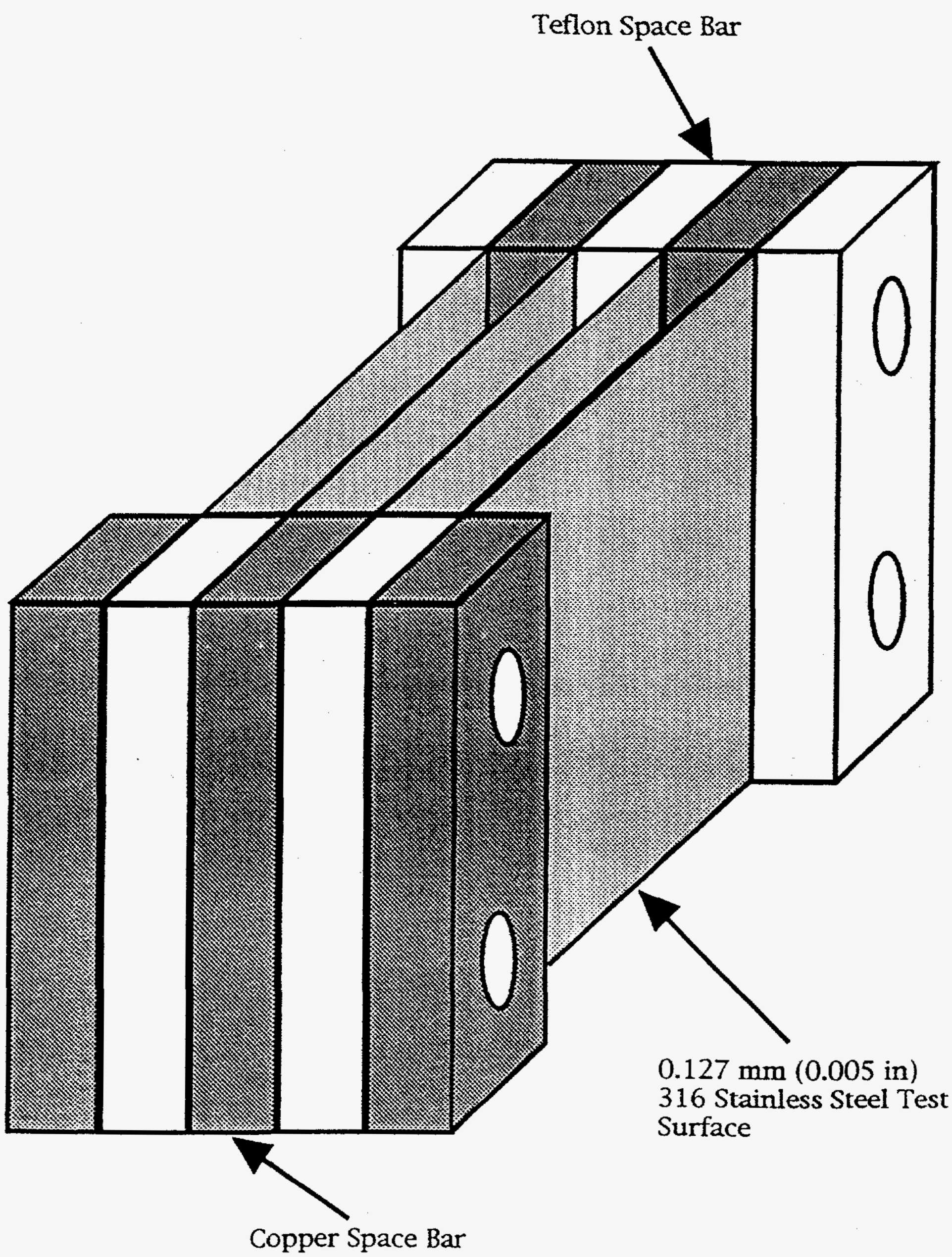


**Figure 3 Typical Surface Test Assembly**

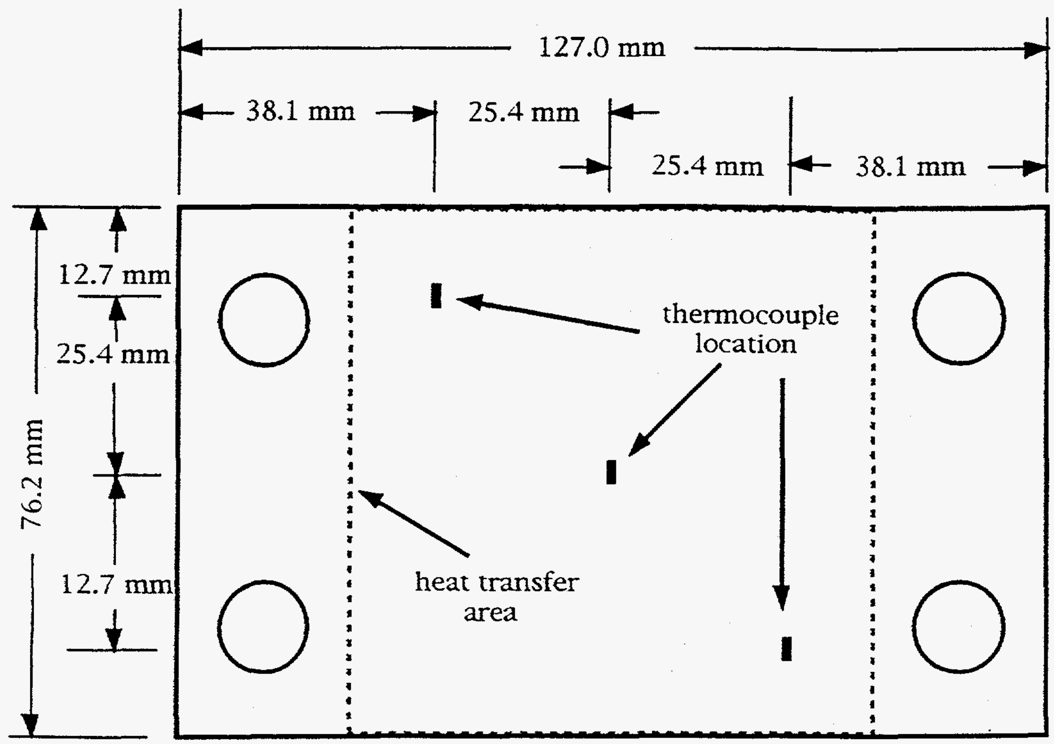


**Figure 4a Thermocouple Locations**

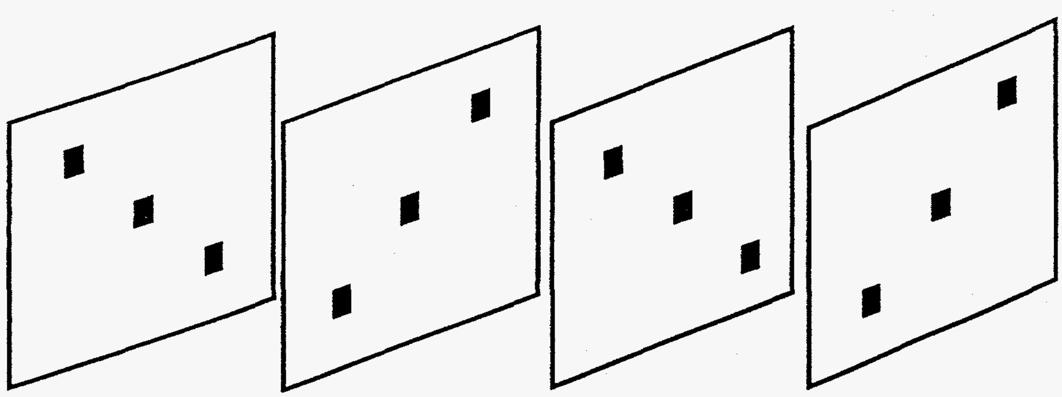

**Figure 4b Illustration of Alternating Thermocouple Pattern**

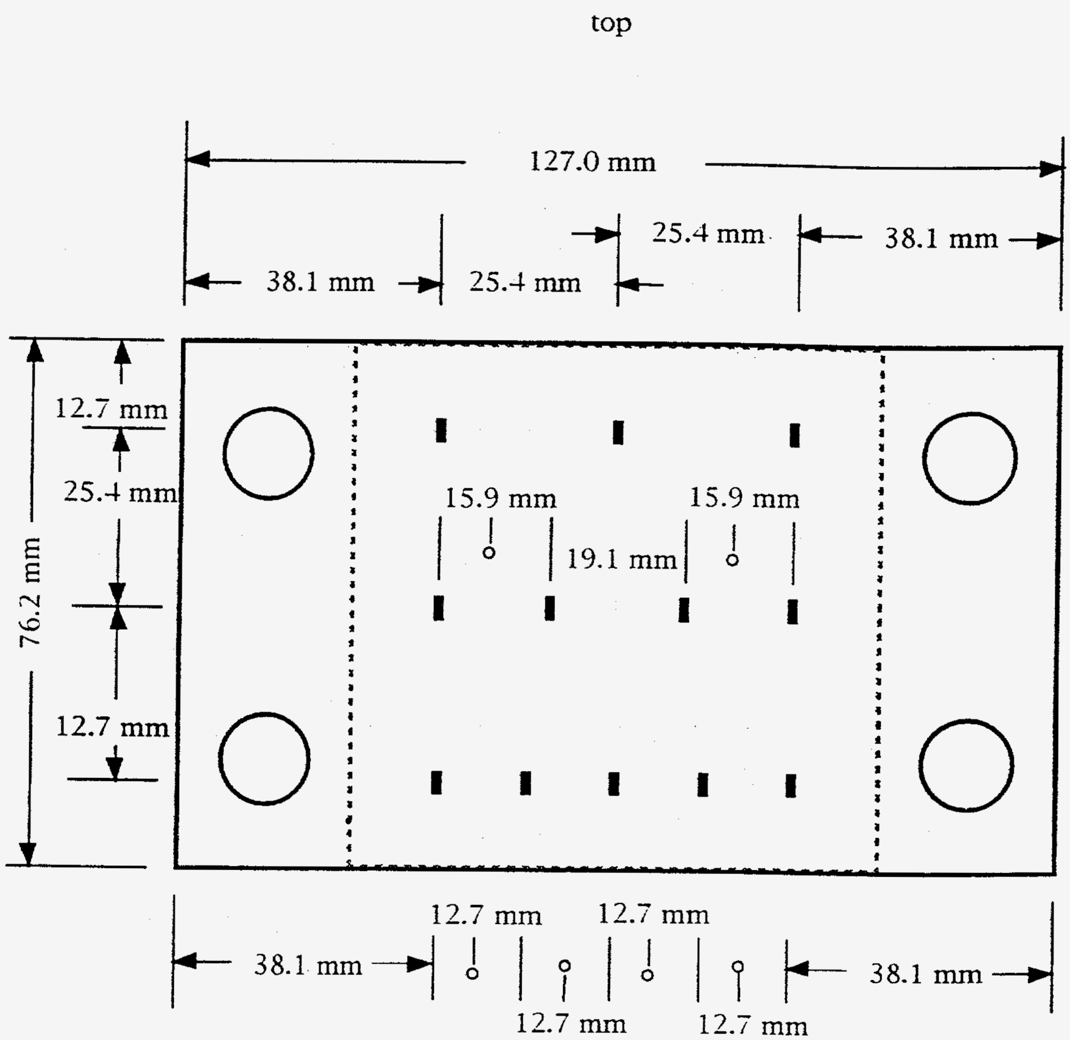


**Figure 5 Single Surface Assembly Thermocouple Locations**

in Table 1. Gravitational forces were not expected to significantly affect flow parameters such as the droplet breakup velocity.

**Table 1 Summary of test variables and Freon-113 properties**

| Variable | Range |
|---|---|
| Liquid flow rate | $9.46\ cm^3\ s^{-1}$ - $126.18\ cm^3\ s^{-1}$ |
| Nozzle orifice diameter, d | 1.19 mm - 3.57 mm |
| Nozzle to test surface distance, x | 0.211 - 0.241 m |
| Droplet breakup velocity, v | $5.0 - 29.0\ m\ s^{-1}$ |
| Droplet diameter, $d_p$ | 200 - 950 μ m |
| Test surface temperature, $T_w$ | 4 - 65 °C |
| Liquid temperature, $T_l$ | 2 - 10 °C |
| Heat flux, q" | $1{,}000 - 130{,}000\ W\ m^{-2}$ |
| Surface separation distance, gap | 6.35 - 25.4 mm |
| Liquid density, $\rho_l$ | $1{,}575 - 1{,}625\ kg\ m^{-3}$ |
| Vapor density, $\rho_v$ | $1.28 - 2.45\ kg\ m^{-3}$ |
| Viscosity, μ | $7.435e-4 - 9.345e-4\ N\ s\ m^{-2}$ |
| Surface tension, σ | $0.017 - 0.022\ N\ m^{-1}$ |
| Latent heat, $h_{fg}$ | $144{,}650 - 146{,}800\ J\ kg^{-1}$ |
| Specific heat, $c_l$ | $895 - 921\ J\ kg^{-1}\ °C^{-1}$ |
| Weber Number, $\rho_l\ v^2\ d_p\ \sigma^{-1}$ | 2,000 - 15,000 |

## Heat Flux

Heat fluxes across each test section were assumed uniform because the thickness of the stainless steel test surfaces on which the electrical resistances depend varied by less than two percent. Therefore, local and average surface heat flux values were assumed constant across each surface. The electrical current that flowed through all of the test surfaces was determined by measuring the voltage drop across a 10 Ohm shunt type precision resistor used in conjunction with a current transformer. Separate voltage drop measurements were taken for each test surface. Heat flux values in each test surface were calculated by

$$q''_{power} = \frac{e\left(\frac{1200}{5}\frac{E}{R_p}\right)}{A} \tag{1}$$

where e is the measured voltage drop across each test surface, E is the measured voltage drop across the precision resistor, $R_p$ is the resistance of the precision resistor, 1200/5 is the current transformer ratio, and A is the heat-transfer area. The total heat flux for a test surface was defined as

$$q'' = q''_{power} - q''_{conduction} - q''_{radiation} \tag{2}$$

where $q''_{power}$ is defined by equation (1), $q''_{conduction}$ is the conduction loss, and $q''_{radiation}$ is the radiation loss. An analysis of the conduction and radiation losses indicated the combined losses were less than three percent, based on the maximum power. Therefore, conduction and radiation losses were not included in the data analysis portion of this research.

## Temperature Definitions

The average wall temperature, $T_w$, is useful in characterizing the heat transfer. The local surface temperatures, $T_x$, were averaged for each heated surface to form the wall temperature, defined as

$$T_w = \frac{1}{n} \sum_{i=1}^{n} T_{x,i} \tag{3}$$

The film temperature, $T_f$, was defined as the average of the wall temperatures, $T_w$, and the liquid Freon-113 spray temperature, $T_l$.

$$T_f = \frac{T_w + T_l}{2} \tag{4}$$

## Freon-113 Properties

Freon-113 properties were obtained from E. I. du Pont de Nemours and Company (1938), E. I. du Pont de Nemours and Company (1963), E. I. du Pont de Nemours and Company (1967), E. I. du Pont de Nemours and Company (1973), and Stewart et al. (1986). All of the properties, except for the latent heat, were evaluated at the film temperature, $T_f$. The latent heat, $h_{fg}$, was evaluated at the saturation temperature based on the absolute chamber pressure.

## Spray Parameters

The droplet diameter, surface tension, and droplet breakup velocity play important roles in characterizing the impact of a spray on a surface. Although techniques such as laser-Doppler anemometry are capable of directly measuring the droplet diameter breakup velocity, empirical equations provide sufficient accuracy and have been successfully used in previous work (e.g. Longwell, 1956; Bonacina et al., 1979; Ghodbane, 1988; Holman and Kendall, 1993) to determine these parameters. In addition, pressure atomizing full cone type nozzles produce a range of droplet diameters and velocities for each specific pressure differential. Therefore, the empirical correlations provide average spray parameter values based on measurable experimental parameters.

The mass median diameter, defined as the size of droplet at which the mass of a sample of spray is divided into two equal parts, was used to define the droplet diameter. Equation (5), which was presented by Bonacina et al. (1979) defines the mass median diameter based on flow parameters.

$$d_p = \frac{9.5d}{\Delta p^{0.37} \sin(\beta/2)} \tag{5}$$

In equation (5), the droplet diameter, $d_p$, has the same units as the diameter of the nozzle orifice, d, $\Delta p$ is the difference in the nozzle and chamber pressures in units of Pascals, and $\beta$ is the spray cone angle. Droplet diameters vary considerably for different nozzle orifice diameters and pressures. Typical droplet diameters ranged from 200 $\mu$m to 950 $\mu$m.

Freon-113 surface tension values were calculated using the Macleod-Sugden correlation, presented in Reid et al. (1987) as

$$\sigma = \left( \frac{P}{M} (\rho_l - \rho_v) \right)^4 \tag{6}$$

where the surface tension, $\sigma$, is in dyn $cm^{-1}$, the liquid and vapor densities, $\rho_l$ and $\rho_v$, are in g $cm^{-3}$, the parachor, P= 249.6 $cm^3$ $g^{0.25}$ $s^{-0.5}$ $mol^{-1}$, and the molecular weight, M, is in g $mol^{-1}$.

Droplet breakup velocities were calculated based on an energy balance for a control volume, presented in Ghodbane and Holman (1991) as

$$v = \left( v_l^2 + \frac{2\Delta p}{\rho_l} - \frac{12\sigma}{\rho_l d_p} \right)^{1/2} \tag{7}$$

where $v_l$ is the liquid velocity in the tube prior to the nozzle. The derivation of equation (7) assumed negligible gravity effects, negligible air and vapor circulation effects, constant density, and a uniform pressure at the control volume outlet. A simplified energy equation was obtained using the number of droplets as a parameter. By solving for the number of droplets in the continuity equation and substituting into the simplified energy equation, equation (7) was obtained.

## Correlation Parameters

The Weber number, We, has been shown to play a role in spray cooling, and is defined in this application as

$$We = \frac{\rho_l d_p v^2}{\sigma} \tag{8}$$

where the liquid density, $\rho_l$, droplet diameter, $d_p$, droplet breakup velocity, v, and surface tension, $\sigma$, are defined above. Droplet impact dynamics are dependent on the Weber number. Because the heat-transfer characteristics of spray cooling are dependent on the heat flux to impacting droplets, spray cooling heat-transfer will also be dependent on the Weber number. Both single droplet heat-transfer research (Holman et al., 1972) and spray cooling research (Choi and Yao, 1987; Ghodbane, 1988) have identified the Weber number as a parameter in describing the heat-transfer process; therefore, it was expected to play a role in describing spray cooling heat-transfer for the VCHF surfaces.

Another parameter used in the description of spray cooling is the mass flux, defined as the mass flow rate divided by the cross-sectional spray flow area. The distance from the nozzle to the heated surface is a geometric parameter which may be indicative of the surface mass flux. Ghodbane (1988) and Holman and Kendall (1993) successfully used the distance from the nozzle to the heated surface in correlating heat-transfer results for normally impacting sprays, and this distance was expected to play a similar role and improve correlations for the VCHF surfaces.

## Uncertainty Analysis

Uncertainty analyses of all experimental measurements were performed using a method described by Kline and McClintock (1953). The most pertinent parameter uncertainties were a heat flux uncertainty of 0.071 W $m^{-2}$, temperature uncertainty of 1.4°C, droplet breakup velocity uncertainty of 0.038 m $s^{-1}$, latent heat uncertainty 329.4 J $kg^{-1}$, dynamic viscosity uncertainty of 2.02E-5 N s $m^{-2}$, and a film temperature uncertainty of 0.7°C.

# EXPERIMENTAL RESULTS AND DISCUSSION

Normally impacting spray cooling with subcooled Freon-113 was successfully correlated by Ghodbane (1988) using an equation of the form

$$\frac{q''x}{\mu h_{fg} We^{0.60}} = B\left[\frac{c_l(T_w - T_l)}{h_{fg}}\right]^{\gamma} \tag{9}$$

Following the same methodology, initial efforts to correlate the present data focused on averaging the heat fluxes and wall temperatures for all of the test surfaces in an assembly and applying the correlation parameters in equation (9). The average heat flux and average wall temperature will be referred to as $q''_{avg}$ and $T_{w,avg}$ respectively. Averaging these values seemed reasonable because local and average heat-transfer behaviors were the same in Ghodbane (1988), symmetry about the axial centerline of the spray was maintained, and variations along the vertical axis of the test surfaces are expected to be linear as a result of the linear relationship with the distance from the nozzle to the heated surface, x. In addition, average heat transfer correlations can be useful in practical engineering applications.

When all of the average heat-transfer data from the present study are plotted using the parameters in equation (9) and using the method of least-squares in conjunction with visual observations of the graph, a nondimensional correlation was found to follow a semi-log form

$$\frac{q''_{avg}\, x}{\mu h_{fg} We^{0.60}} = 0.181 + 0.107 \log\left[\frac{c_l(T_{w,avg} - T_l)}{h_{fg}}\right] \tag{10}$$

Figure 6 presents the "averaged" data (average of all surfaces in an assembly) plotted with a line calculated by equation (10). Surface spacing distances are not delineated because the graph would become overly complicated. One may state, however, that the average heat-transfer correlation for the VCHF assemblies was essentially independent of the surface spacing. The semi-log form of equation (10) was unexpected. Normally impacting spray cooling by Ghodbane (1988) and Holman and Kendall (1993) as well as unpublished results of spray cooling through two parallel vertical constant heat flux surfaces indicate that the parameters of equation (9) should lead to a log-log cooling curve profile. The semi-log form of equation (10) suggests that another parameter not revealed in previous research is present.

The heat-transfer behavior of individual surfaces in each assembly was also evaluated using the correlation parameters in equation (9) to determine if the semi-log curve was a result of the averaging. Heat fluxes and wall temperatures for individual surfaces were determined by equation (1) and equation (3) respectively. When the correlated data were plotted for the surfaces of each VCHF assembly, a dependence on the distance from the axial centerline of the spray was evident. The outer surfaces conform to the log-log cooling curve seen in normally impacting sprays (equation (9)), while the surfaces closer to the axial spray centerline exhibit a semi-log cooling behavior. To confirm and evaluate this behavior, another set of experiments were performed with the single surface assembly located at various distances from the axial centerline of the spray.

Heat-transfer data from a single vertical constant heat flux surface were acquired for horizontal distances from the axial centerline of the spray equal to 0.00 mm, 6.35 mm, 12.70 mm, 19.05 mm, and 31.75 mm using one nozzle with a fixed nozzle to surface distance, x, and flow rates ranging from 59.94 cc/sec to 100.9 cc/sec. When the data are plotted using the parameters of equation (9), the dependence on the horizontal distance from the axial centerline of the spray is very apparent, as illustrated in Fig. 7. The cooling curves change from log-log to semi-log form when the distance from the axial centerline is less than 19.05 mm. Thus, the test surfaces close to the axial spray centerline exhibit the semi-log type behavior. Because the data correlation in Fig. 6 uses overall average heat-transfer rates for all surfaces in the assembly, the functional form of the average data is affected by the semi-log behavior of the inner surfaces close to the centerline of the spray.

Local heat-transfer behavior on each heated surface was also dependent on the distance from the axial centerline of the spray. Surfaces with distances from the axial centerline greater than 12.7 mm exhibit identical local and average heat-transfer behaviors, following a power-law relation like equation (9). On the other hand, surfaces with distances from the axial centerline less than 12.7 mm have different cooling

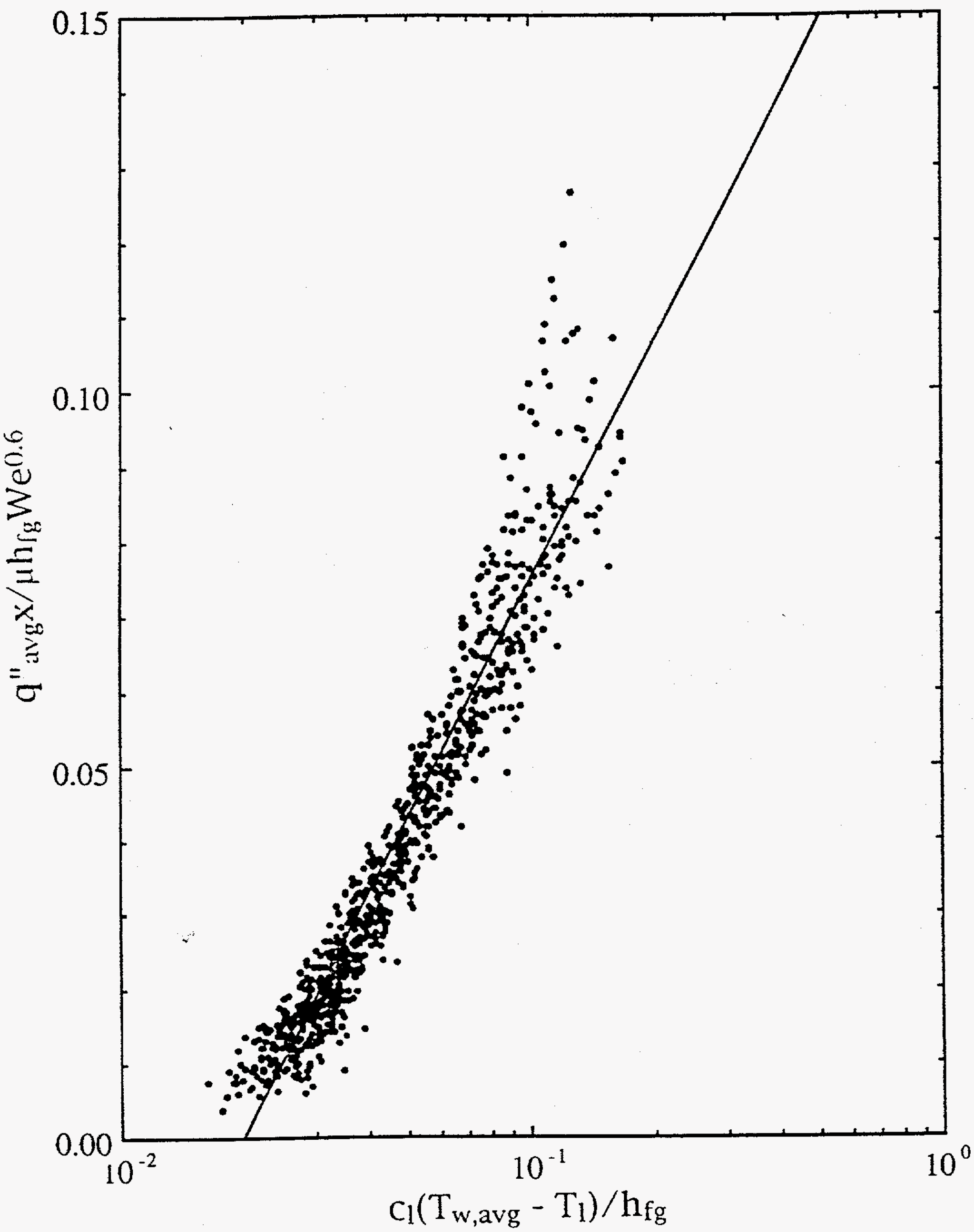


**Figure 6 Correlated "Averaged" Data**

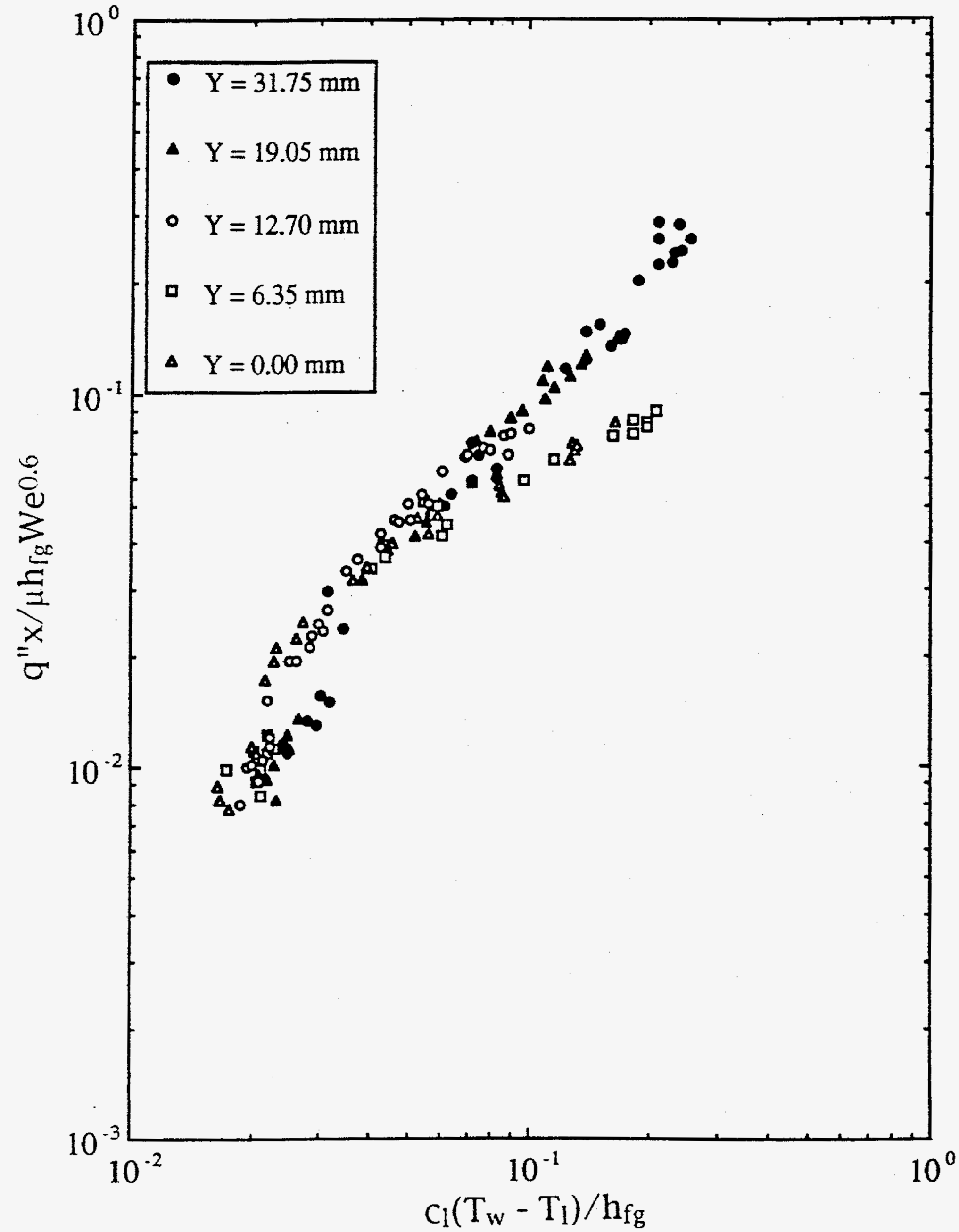


**Figure 7 Correlated Data with Individual Surfaces Distinguishable by Their Distance from the Axial Centerline of the Spray**

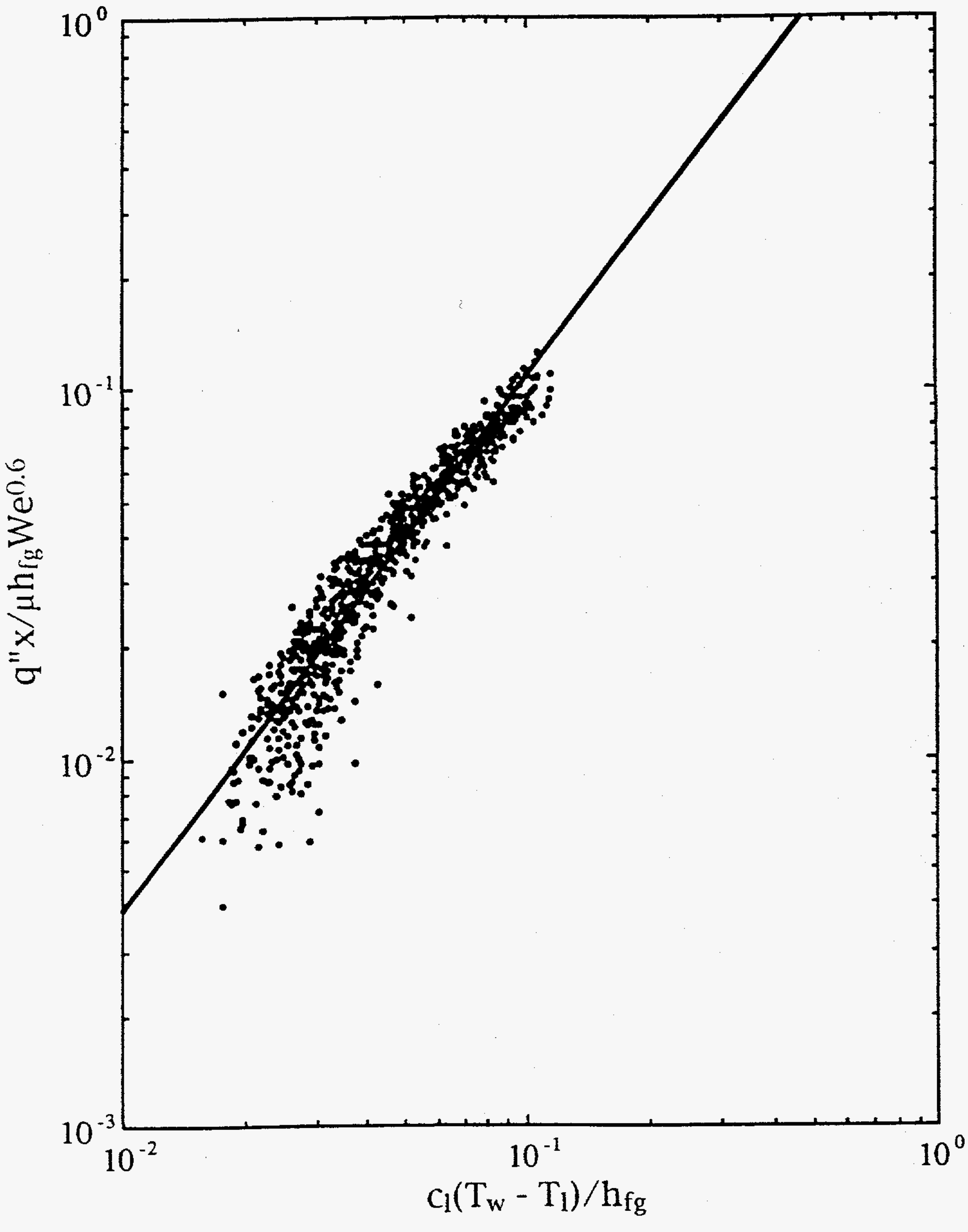


**Figure 9 Correlated Data for Surfaces with Distances from the Axial Centerline of the Spray Greater Than 12.7 mm**

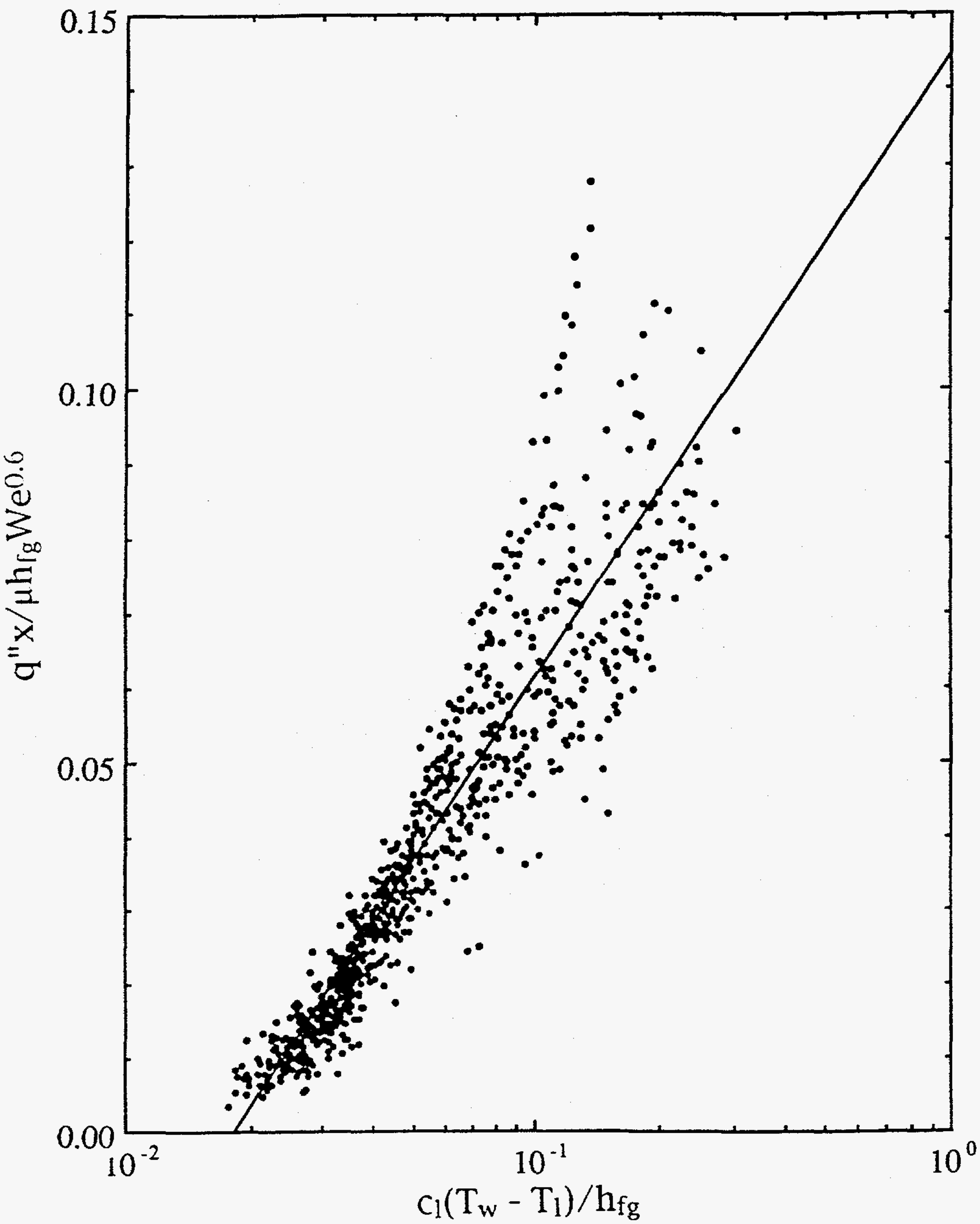


**Figure 10 Correlated Data for Surfaces with Distances from the Axial Centerline of the Spray Less Than 12.7 mm**

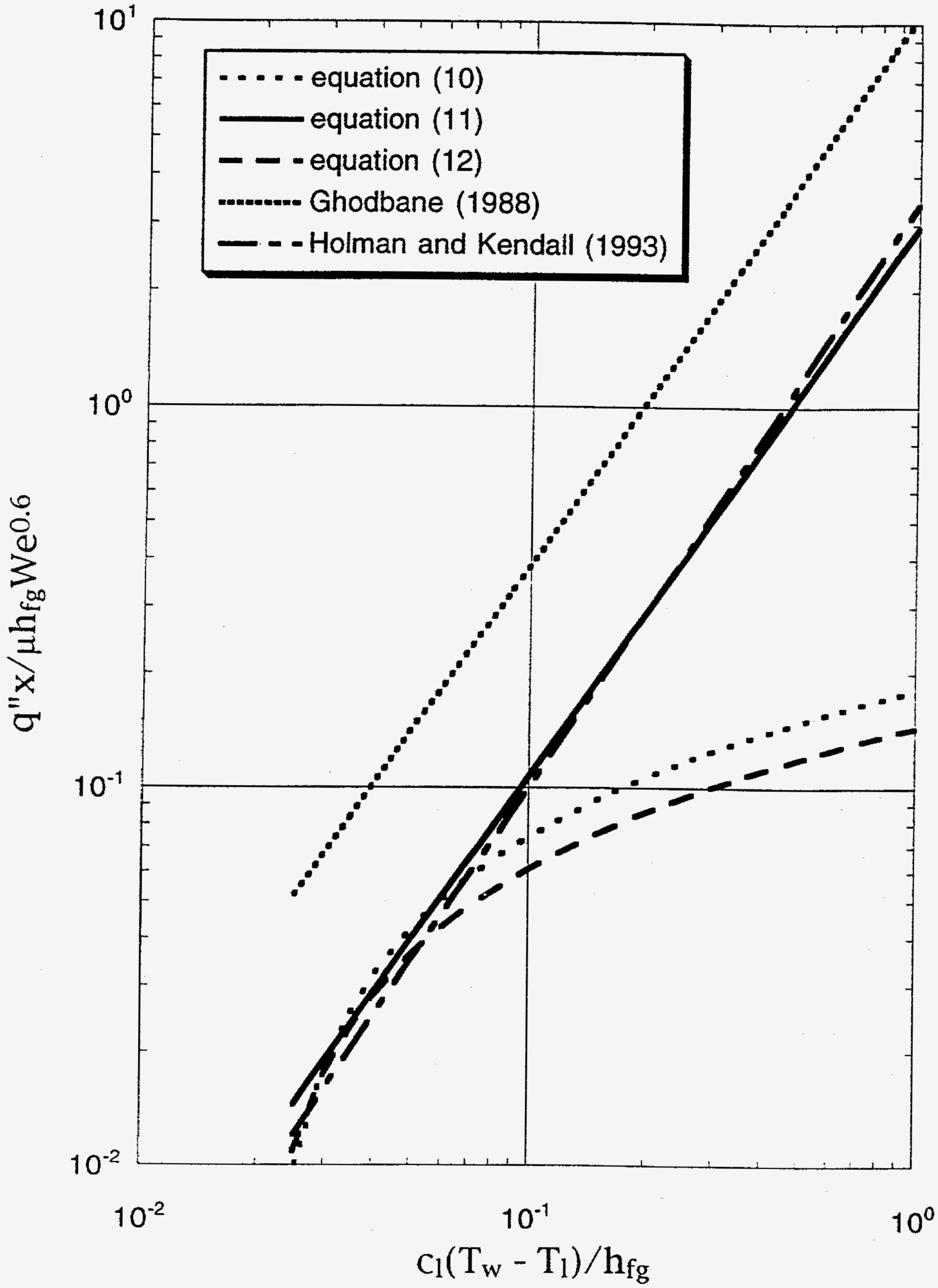


**Figure 11 Comparison of Correlation Equations (10, 11, 12) with Heat-Transfer Correlations for Normal-Impact Spray Cooling**

and compared with the normal-impact spray cooling heat-transfer correlations by Ghodbane (1988) and Holman and Kendall (1993).

The amount of subcooling may contribute to the different ordinate intercepts of the three log-log form correlation equations in Fig. 3. Ghodbane (1988) demonstrated that the amount of subcooling affects the constant term, B, in equation (9), thus affecting the locus of the ordinate intercepts. The semi-log curves of equations (10 and 12) are also affected by the amount of subcooling. Unfortunately, the functional relationship between the amount of subcooling and the correlation equation constants is not known. Future investigations designed specifically to evaluated this effect are recommended. In addition, future experiments should also utilize different fluids to corroborate the non-dimensional correlation equations presented.

## CONCLUSIONS

The heat-transfer characteristics of subcooled Freon-113 sprays generated by pressure atomizing full-cone type nozzles in parallel vertical constant heat flux surfaces were investigated including the effect of the distance from the axial centerline of the spray. Based on the experimental results, the following conclusions were obtained:

1. Local spray cooling heat-transfer for surfaces parallel to the flow is dependent on the location of the surface relative to the axial centerline of the spray.
2. A nondimensional correlation for the overall average heat-transfer was determined to have the form

$$\frac{q''_{avg}\,x}{\mu h_{fg} We^{0.60}} = 0.181 + 0.107 \mathrm{Log}\left(\frac{c_l\left(T_{w,avg} - T_l\right)}{h_{fg}}\right)$$

   This correlation is essentially independent of the surface separation distances for the distances tested, but does not accurately predict the local heat-transfer behavior.

3. For surface distances from the axial centerline of the spray greater than 12.7 mm, data are correlated using a power-law relation successfully used in normally impacting sprays:

$$\frac{q''x}{\mu h_{fg} We^{0.60}} = 2.94\left(\frac{c_l\left(T_w - T_l\right)}{h_{fg}}\right)^{1.44}$$

   This correlation is useful for both the local and average heat transfer behaviors.

4. For surfaces less than 12.7 mm from the axial centerline of the spray, data are correlated using

$$\frac{q''x}{\mu h_{fg} We^{0.60}} = 0.144 + 0.083 \log\left[\frac{c_l(T_w - T_l)}{h_{fg}}\right]$$

   Different local heat transfer behavior was observed in the direction of the flow.

## ACKNOWLEDGMENTS

This study was financially supported by the Brown Foundation Chair in the Mechanical Engineering Department at Southern Methodist University. This work was, in part, performed under the auspices of the U.S. Department of Energy by Lawrence Livermore National Laboratory under contract no. W-7405-Eng-48.

## REFERENCES

Bonacina, C., Del Giudice, S., and Comini, G., 1979, "Dropwise Evaporation", *ASME Journal of Heat Transfer, Vol.* 101, pp. 441 - 446.

Chang, J.M., Tilford, T., Pais, M.R., Morgan, M., and Chow, L.C., 1993, "Spray Cooling of Tuna-Fish-Can Size High Performance Electronic Multi-Chip Modules, ASME Paper 93-HT-19.

Choi, K.J., and Yao, S.C., 1987, "Mechanisms of Film Boiling Heat Transfer of Normally Impacting Spray," *International Journal of Heat and Mass Transfer* , Vol. 30, No. 2, pp. 311-318.

E. I. du Pont de Nemours and Company, 1938, "Thermodynamic Properties of Freon-113, Trichlorotrifluoroethane, $CCl_2F$-$CClF_2$, with Addition of other Physical Properties", T-113A, DuPont Technical Bulletin , Wilmington, Delaware.

E. I. du Pont de Nemours and Company, 1963, "Surface Tension of the Freon Compounds", D-27, DuPont Technical Bulletin, Wilmington, Delaware.

E. I. du Pont de Nemours and Company, 1967, "The Viscosities of Freon Refrigerants", B-10A, DuPont Technical Bulletin, Wilmington, Delaware.

E. I. du Pont de Nemours and Company, 1973, "Transport Properties of Fluorocarbons", C-30, DuPont Technical Bulletin , Wilmington, Delaware.

Ghodbane, M., 1988, "Experimental Study of Spray Cooling with Freon-113", Ph.D. Dissertation, Southern Methodist University, Dallas, Texas.

Ghodbane, M., and Holman, J.P., 1991, "Experimental Study of Spray Cooling with Freon-113," *International Journal of Heat and Mass Transfer* , Vol. 34, pp. 1163 - 1174.

Holman, J.P., Jenkins, P.E., and Sullivan, F.G., 1972, "Experiments on Individual Droplet Heat Transfer Rates," *International Journal of Heat and Mass Transfer* , Vol. 15, pp. 1489-1495.

Holman, J.P., and Kendall, C.M., 1993, "Extended Studies of Spray Cooling with Freon-113," *International Journal of Heat and Mass Transfer* , Vol. 36, pp. 2239 - 2241.

Kline, S.J., and McClintock, F.A., 1953, "Describing Uncertainties in Single-Sample Experiments," *Mechanical Engineer*, January, pp. 3.

Longwell, J.P., 1956, "Combustion of Liquid Fuels," Combustion Processes, Princeton Univ. Press, pp. 407-415.

Simmons, H.C., and Harding, C.F., 1981, "Some Effects of Using Water as a Test Fluid in Fuel Nozzle Spray Analysis," *Journal of Engineering for Power* , Vol. 103, pp. 118 - 123.

Reid, R. C., Prausnitz, J. M., and Poling, B. E., 1987, The Properties of Gases and Liquids (4th Edn), pp. 600 - 601, McGraw-Hill, New York.

Rothe, P.H., and Block, J.A., 1977, "Aerodynamic Behavior of Liquid Sprays," *International Journal of Multiphase Flow* , Vol. 3, pp. 263 - 272.

Sehembey, M.S., Pais, M.R., and Chow, L.C., 1992, "A Study of Diamond Laminated Surfaces in Evaporative Spray Cooling," *Thin Solid Films*, Vol. 212, pp. 25-29.

Stewart, R.B., Jacobson, R.T., and Penoncello, S.G., 1986, Thermodynamic Properties of Refrigerants, American Society of Heating, Refrigerating and Air Conditioning Engineers, Inc. (ASHRAE), Atlanta, Georgia.

Tilton, D.E., Tilton, C.L. Pais, M.R., and Morgan, M.J., 1992, "High-Flux Spray Cooling in a Simulated Multiple Module," ASME Paper No. HTD-Vol. 206-2, Vol. 2, pp. 73-79.